INSTITUTE OF PHYSICS PUBLISHING MEASUREMENT SCIENCE AND TECHNOLOGY

Meas. Sci. Technol. **16** (2005) 2511–2516 doi:10.1088/0957-0233/16/12/016

Production of a 10 eV–1000 eV neutral particle beam using surface neutralization

Martin Wieser and Peter Wurz

Physikalisches Institut, University of Bern, Sidlerstrasse 5, 3012 Bern, Switzerland

E-mail: wurz@phim.unibe.ch

Received 14 April 2005, in final form 3 October 2005
Published 15 November 2005
Online at stacks.iop.org/MST/16/2511

Abstract

For the calibration of low-energy neutral particle mass spectrometers a neutralization stage for a charged-particle beam was built. The incident positive ion beam is neutralized upon reflection at grazing incidence off a highly polished tungsten single crystal surface. With protons as primary species the device produced a neutral hydrogen beam in the energy range of 10 eV–1000 eV depending on incident ion-beam energy with a centre energy of 85% to 89% and an energy width of 11% to 15% FWHM of the incident ion energy. The angular spread of the neutral beam was limited by apertures to 4.6° × 18° FWHM. The overall transmission of the device was found to be between 0.005 and 0.013.

Keywords: neutral atom beam, surface neutralization, calibration of neutral particle mass spectrometers

Introduction

Measurements of the physical parameters (temperature, density, composition, and others) of the local interstellar medium (LISM) will give information about the evolution of the solar system and our galaxy. The LISM is separated from the solar system by the heliopause and charged interstellar particles cannot cross this boundary to enter the solar system. The neutral fraction of the LISM, however, is not subject to magnetic interactions and can therefore penetrate deeply into the solar system. As the Sun moves with a velocity of approximatively 26 km s^{-1} relative to the LISM, a directed inflow of interstellar neutral atoms can be observed [1–3]. Furthermore, energetic neutral atoms (ENA) are produced by charge exchange processes at the heliospheric boundary [4] revealing information about the global structure of the heliosphere.

When approaching the Sun the neutral atom populations are affected by gravitation, photoionization and charge exchange processes. For a spacecraft travelling from Earth toward the heliopause, at a distance of more than about four astronomical units from the Sun these effects become negligible. Consequently it is possible to infer the properties of the neutral interstellar gas and its interaction with the heliosphere by measuring the properties of the inflowing energetic neutral atoms [5]. This has been done for interstellar helium by the Neutral Interstellar Gas Instrument (GAS) on the ULYSSES spacecraft [6]. Even as close as one astronomical unit to the Sun, a fraction of the neutral particle population survives and can be measured by an instrument in Earth's orbit. In Earth's orbit the energies of such energetic neutral particles range from 10 eV to several 100 eV depending on the location of the Earth with respect to the interstellar gas flow direction and the inflowing species. Such an instrument is presently in operation on board the IMAGE satellite [7]. A next generation low-energy neutral atom mass spectrometer has recently been selected for the Interstellar Boundary Explorer mission (IBEX) of NASA [8].

The calibration of such low-energy neutral atom mass spectrometers requires well-characterized energetic neutral atom beams in the energy range of 10 eV–1000 eV per atom. The calibration system for mass spectrometers (CASYMS) facility [9] and the calibration facility for solar wind instrumentation (MEFISTO) [10], both at the University of Bern, provide well-collimated ion beams in the energy range of interest but do not have a beam neutralization stage. We have built and characterized a portable ion-beam neutralizer compatible with both calibration facilities, MEFISTO and CASYMS.

Charge exchange

Three different approaches to neutralizing an ion beam are reported in the literature. A widely used method is to use

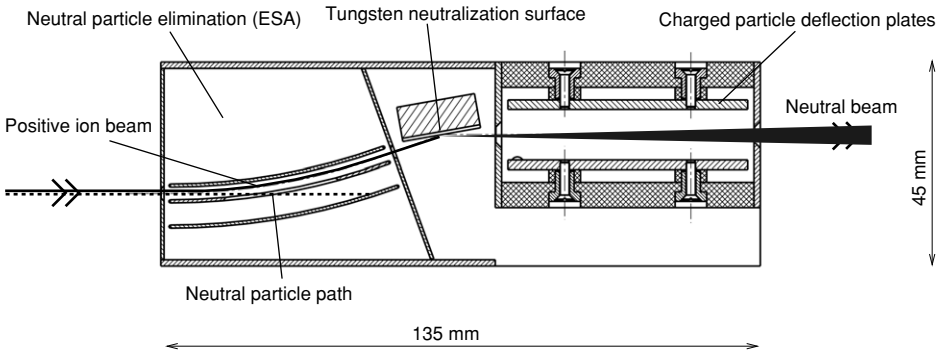

Figure 1. Ion-beam neutralizer. Positive ions enter the system from the left. The electrostatic analyser (ESA) separates any neutrals in the primary beam. Ions are neutralized by reflection at grazing incidence on a polished tungsten single crystal. After reflection, charged particles are removed by the charged-particle deflection system on the right side resulting in a completely neutral particle beam.

charge exchange between an ion beam and a neutral gas. Utterbach and Miller [11] investigated fast molecular nitrogen beams in the energy range of 5–1000 eV. In a charge exchange cell, an energetic ion, $A^+_{\rm fast}$, collides with a thermal, room temperature, neutral gas atom or molecule, B, picking up an electron via

$$A^+_{\rm fast} + B \rightarrow A_{\rm fast} + B^+$$

resulting in $A_{\rm fast}$ exiting the cell as an energetic neutral atom or particle. This is the same process that is responsible for the emission of ENAs from planetary magnetospheres. Neutralization efficiencies up to 10% can be obtained provided suitable charge capture partners can be found. A common implementation consists of a differentially pumped gas cell filled with a noble gas, e.g. xenon, followed by a set of deflection sections to eliminate the remaining ions. The drawback of a gas cell is that it requires differential pumping as the pressure in the gas cell needs to be much larger (10^{-5} mbar) than the pressure in the instrument test chamber (10^{-7} to 10^{-9} mbar). This results in small apertures for the beam for entering and exiting the gas cell and thus also results in a small neutral particle beam diameter.

Photodetachment

Another elegant way to produce a neutral beam is to photodetach an electron from negatively charged ions [12]. Photodetachment is realized with a strong argon-ion laser (kW power level). As an example, ground state O(^{3}P) is produced from O^- using photons with an energy of less than 3.43 eV. Neutralization rates of the per cent level are obtained with the available kW laser power. Remaining ions are removed electrostatically. Neutral atom beams of hydrogen and oxygen in an energy range of 4–1000 eV with an energy spread of 1.5 eV given by the ion source have been realized. However, the photodetachment technique is limited to species that form stable negative ions and requires a negative ion source. Furthermore the need of a laser in the kW power range imposes additional complications.

Surface neutralization

A third way to produce a neutral particle beam is to use surface neutralization. When ions are scattered off solid surfaces at grazing incidence, specular reflection of the incoming ion beam will occur if the surface is flat on an atomic scale. In addition, charge-exchange reactions between the projectile and a metal surface take place, especially Auger neutralization, resonance neutralization and quasi-resonant processes, resulting in an efficient neutralization of the scattered particle [13]. A small deflection angle guarantees that a sufficiently long time for charge exchange is available. Large neutralization rates (>90%) may be obtained this way. This technique for production of energetic neutral atoms is also used in surface science experiments [14]. Recently, Losch and Niehus [14, 15] used a Pt(1 1 1) surface to convert an ion beam into a neutral atom beam for surface science studies in an UHV environment. They used grazing incidence at 4.5° for particle scattering. The energy loss was about 100 eV with an energy spread of <40 eV for 3 keV He scattered from a Pt single crystal. Larger angles will cause more energy loss and increased energy and angular scatter.

Despite the energy loss, energy and angular scatter introduced by the scattering surface, surface neutralization was chosen to build a neutralization device because it has several advantages compared to other methods of neutralizing an ion beam. It does not require an additional pumping system and the neutralization device may be put into the beam line as an additional unit without modifications to the vacuum system. Apart from some high voltages, no additional feedthroughs out of the vacuum chamber are needed. The neutralizer operates under the same conditions as the instrument under test, can be built sufficiently small and may be easily installed in both facilities, MEFISTO and CASYMS.

Neutralizer

Figure 1 shows a cross-sectional drawing of the ion-beam neutralizer. It consists of an electrostatic analyser, a scattering surface, a set of apertures and an ion deflection system. Figure 2 shows the unit, the rectangular box left of the centre of the image, attached to the IBEX-Lo prototype [16] of the Interstellar Boundary Explorer (IBEX) [8] installed in the MEFISTO calibration facility.

A neutral atom beam is produced by reflection of a low-energy positive ion beam from a single crystal tungsten surface with (1 1 0) surface orientation, polished to better than 0.03 $\mu m_{\rm rms}$. Most ions are neutralized (>90%) and molecules

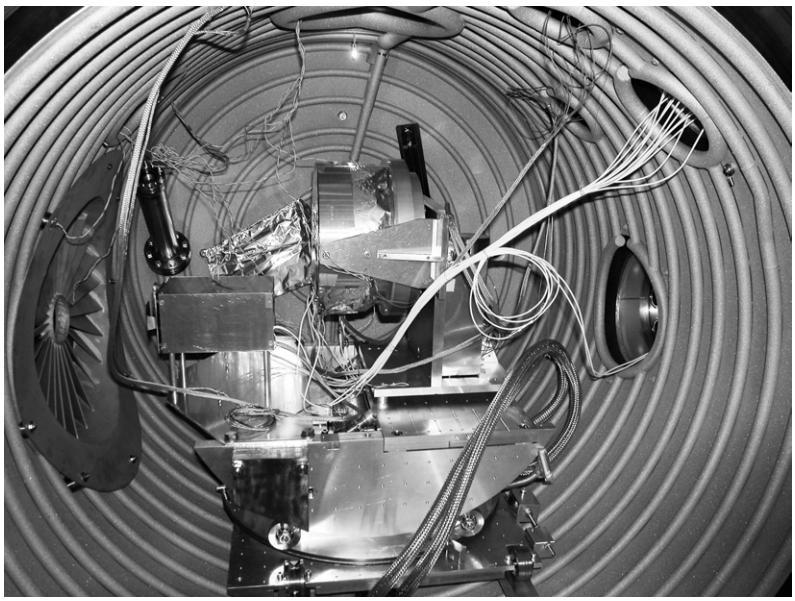

Figure 2. Ion-beam neutralizer, inside the rectangular box left of centre serving as a high voltage shield, installed at the MEFISTO calibration facility of the University of Bern, Switzerland. The ion beam enters the chamber from the left through the fan shaped opening. The installed instrument is the IBEX-Lo sensor prototype [16] of the Interstellar Boundary Explorer mission IBEX [8].

mostly dissociate upon reflection. The latter allows us to use H_2^+ as primary particles to create neutral hydrogen atoms as well. Molecular ions are produced very efficiently in the CASYMS ion source. Hydrogen atoms experience an energy loss of 11%–15% upon reflection. After reflection the remaining charged particles are removed by an electrostatic deflection system. Collimation plates reduce the angular spread of the neutral beam. The result is a divergent neutral beam with a broadened energy distribution.

Possible neutral particles originating from grids in the ion-beam line are absorbed in the electrostatic analyser (ESA) in front of the neutralization surface. This ESA also bends the incident ion beam such that the resulting exiting neutral beam axis is parallel to the incident ion-beam axis. A hole in the lower ESA plate separates incident fast neutral particles such that they do not have the possibility of getting reflected at the outer ESA plate to the exit of the ESA as ions and to broaden the energy distribution of the produced neutrals. For low-energy neutrals (<500 eV) the ion-beam energy from the MEFISTO source was held fixed and the neutralizer box was floated at a variable high voltage instead. With this configuration the primary ion beam intensity and beam profile from the MEFISTO source can be held constant and the neutral beam energy is selected by changing the neutralizer float voltage. The voltage at the ESA plates is adjusted to match the resulting ion energy. Neutral hydrogen beams with centre energies down to 10 eV were produced this way, as successfully verified with the prototype of the IBEX-Lo sensor [16]. The elemental range of the beam neutralizer is not limited to hydrogen; we also investigated other neutral species such as helium, oxygen and neon.

Characteristics

The profile of the neutral beam was measured by placing an imaging micro channel plate (MCP) detector (Quantar Technology Inc., CA, USA, Model 3395A-SE/2401B) at various positions behind the exit of the neutralizer. The beam divergence was 18° FWHM in one direction and collimated down to 4.6° FWHM in the other direction by the exit aperture. A typical beam profile measured using 1 keV He^+ primary ions is shown in figure 3. The transmission of the device was measured for 1 keV He^+ primary ions by comparing the incident ion flux with the neutral flux measured at the MCP detector. The transmission of the device was found to be 0.0054 ± 0.001 at 1 keV, the uncertainty is mostly due to the uncertainty of the detection efficiency of the MCP [17–20]. At lower energies direct measurement of the neutral particle flux becomes increasingly difficult as the detection efficiency of the MCP detector is more and more uncertain. However, since almost all ions are neutralized at the tungsten surface, the change in transmission below 1 keV is determined mainly by the scattering properties of the neutralization surface and is derived from comparisons of the angular scattering images at different energies. Scattering and neutralization properties of

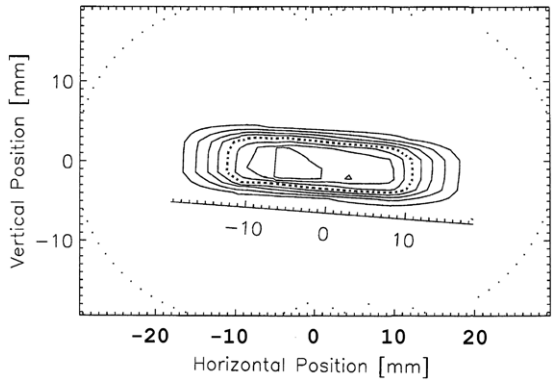

Figure 3. Neutral beam profile at 25 mm distance from the neutralizer exit aperture. The lines are equidistant in intensity, the 63% level is marked as a dotted line.

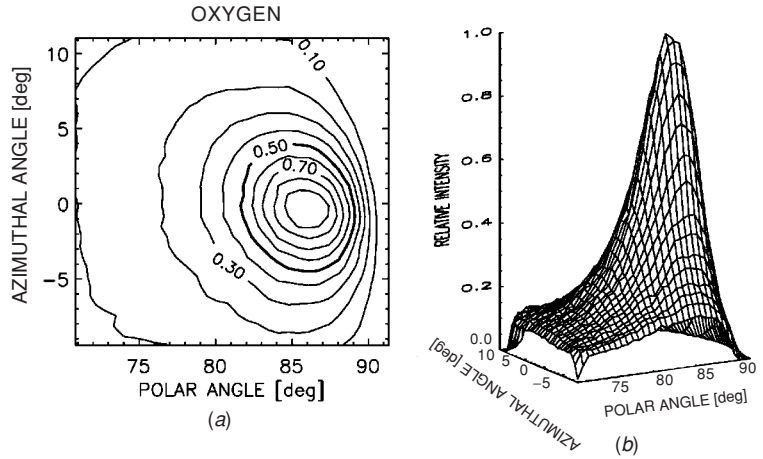

Figure 4. (*a*) Angular scattering profile obtained from scattering 780 eV per molecule O_2^+ off a highly polished W(1 1 0) surface at 82° angle of incidence. (*b*) 3D plot of the same data.

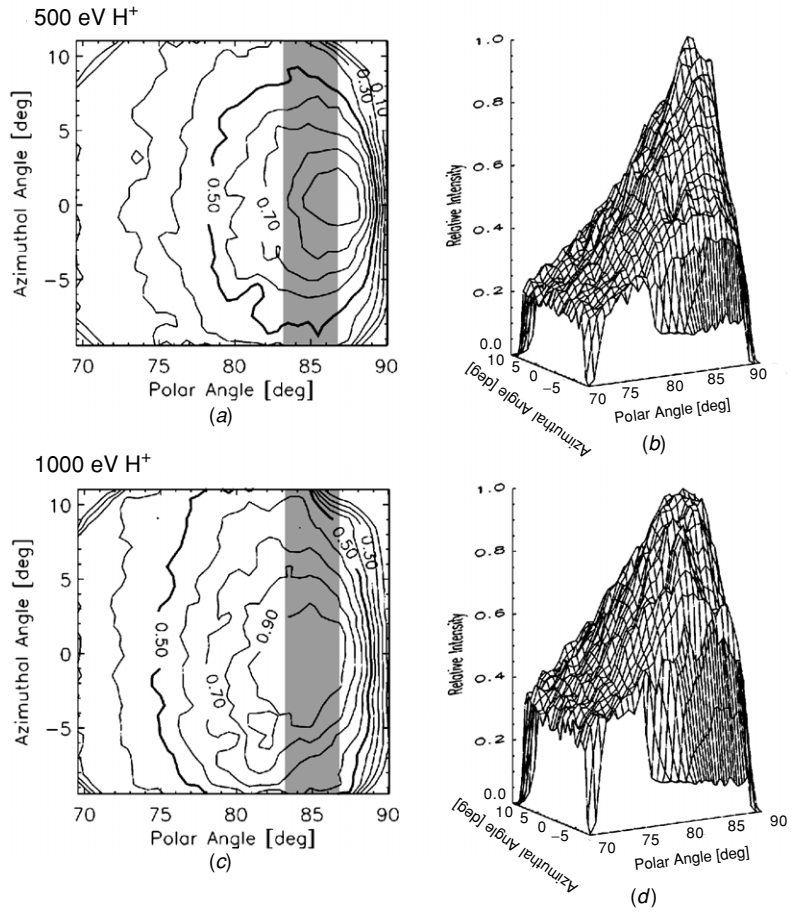

Figure 5. Angular scattering profiles obtained from scattering H^+ ions off an unheated highly polished W(1 1 0) surface at 85° angle of incidence. Data for 500 eV per atom primary energy are shown in (*a*) and (*b*), data for 1000 eV per atom are shown in (*c*) and (*d*). In both cases, the angular scattering is wider than what was obtained from a heated surface as shown in figure 4. The solid angle of acceptance of the charged-particle deflection section is shown as a grey rectangle in the contour plots. At lower energies more particles are scattered into this acceptance region.

the tungsten neutralization surface were measured before in the imager for low-energy neutral atoms (ILENA) facility at the University of Bern [21]. Figure 4 depicts an angular scattering profile of a highly polished tungsten W(1 1 0) surface at an angle of incidence of 82° to the surface normal. This scattering profile is obtained after heating the tungsten surface to more than 1000 °C. As the beam neutralizer unit may be floated to high voltage to decelerate the incoming ion beam, direct heating of the tungsten surface is not available in the present setup. A potential heating circuit would need to be either

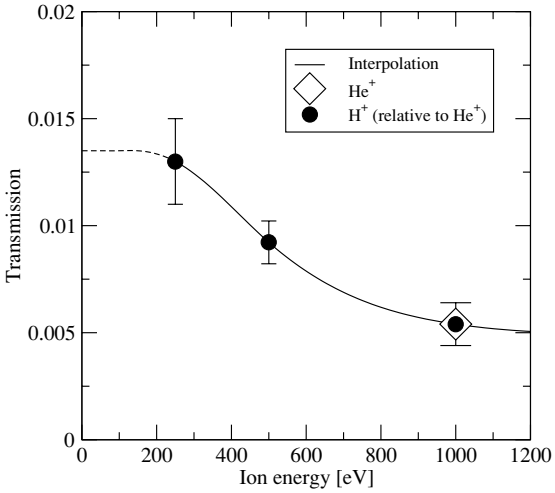

Figure 6. Transmission of the ion-beam neutralizer unit. The value at 1000 eV was measured absolutely using He^+ primary ions. The changes in the shape of the scattering cone obtained from H^+ primary ions were used to calculate the changes in the transmission at lower energies. Below 200 eV the transmission is expected not to increase anymore as most neutral particles are already collected.

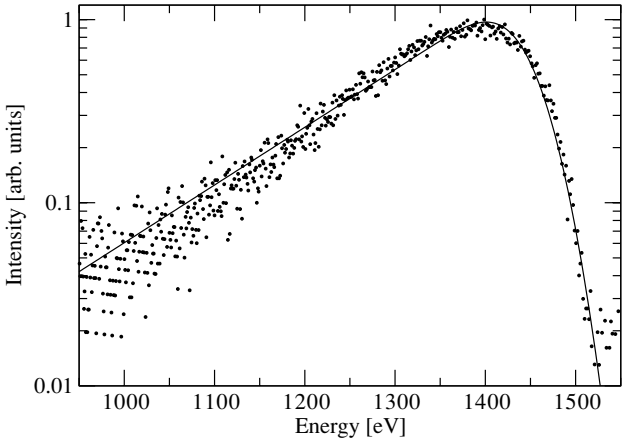

Figure 7. Energy distribution of neutral particles of hydrogen reflected off an unheated tungsten surface derived from a time of flight spectrum. A mono-energetic 1500 eV H^+ primary beam at an incidence angle of 85° to the surface normal was used with the time-of-flight detector placed in the specular reflection direction. The mean energy loss obtained is 11% of the primary energy at a width of the distribution of 11% FWHM of the primary energy. The solid line is a fit to the data and is shown to guide the eye. The shape of the distribution scales approximately with incident particle energy.

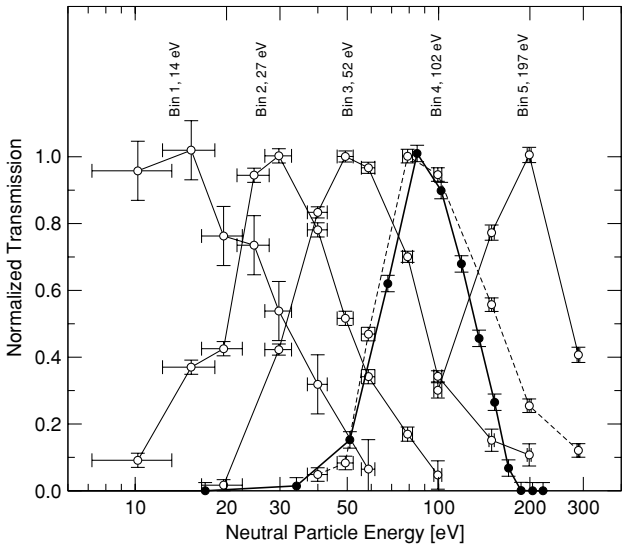

Figure 8. Example of beam neutralizer performance at low energies: response of the IBEX-Lo sensor prototype [8, 16] to incident neutral hydrogen for five energy bins of the IBEX-Lo sensor (open circles). The observed peak width is dominated by the energy resolving power of the sensor. These data do not have the energy distribution of the incident neutral beam deconvolved. The expected theoretical response for a mono-energetic neutral beam is shown for bin 4 (solid circles, bold line). The deviation from the measurement (dashed line) on the high energy side of the peak is due to the energy distribution created at the tungsten surface of the neutralizer. Similar comparisons for the other energy bins show that the energy distribution shown in figure 7 is valid even at the lowest end of the energy range at 10 eV mean neutral particle energy.

electrically insulated from the tungsten surface for operation on ground potential or need to be floated to the neutralizer potential requiring a heater power supply that can be floated up to 3 kV. The unheated tungsten surface results in a broader angular scattering because of the presence of contaminants on the scattering surface which results in a reduced transmission of the device. Also contamination of the neutral beam with low-energy sputtered neutral hydrogen (<50 eV) is possible when creating a neutral beam with more than about 100 eV centre energy. These particles can be identified by pulsing the primary ion beam and using time-of-flight techniques similar to those used in [21]. Also, the tungsten surface may be cleaned by using a high intensity primary ion beam of several 100 eV [22].

The flux into the solid angle of acceptance of the charged-particle deflection section increases for lower energies as shown in figure 5 for an angle of incidence of 85° to the surface normal. The absolute transmission of the complete unit was measured using 1000 eV He^+ primary ions by comparing the primary ion flux with the emerging neutral flux, both measured using the MCP detector. Differences in the detection efficiency between neutrals and positive ions were neglected at this energy. A transmission of 0.0054 ± 0.001 was obtained. The changes in the shape of the scattering cone produced by primary H^+ ions at different energies were used to infer the transmission at lower energies. The narrower scattering cone at lower energies results in an increase of the transmission up to 0.013 at 200 eV as shown in figure 6. At even lower energies the transmission does not increase anymore as most particles are already collected. In floated operation mode, the defocusing of the primary beam in the deceleration stage in front of the neutralizer must carefully be included into the determination of the total transmission.

A typical energy distribution of the neutral particles is shown in figure 7. The neutral energy distribution is asymmetric and has a tail towards lower energies. For 1500 eV primary H^+ ions, an energy loss of 11% and a width of 11% FWHM of the primary energy were found. For hydrogen, the energy distribution of the produced neutrals scales roughly with primary ion energy between 10 eV and 1500 eV incident

ion energy; however at energies below 300 eV the mean energy loss increases to about 15% and the width of the distribution to about 15% FWHM of the incident ion energy. The measured energy distribution is similar to energy distributions obtained with similar geometries from other surfaces [21, 23]. Below 300 eV, the mean and the width of the energy distribution could be verified using the IBEX-Lo sensor prototype [16] as shown in figure 8. In the IBEX-Lo sensor, neutral atoms are ionized by surface ionization and accelerated to keV energies prior to detection by an MCP—thus completely eliminating the problems associated with the decreasing detection efficiency of MCPs below 1 keV. The data shown do not have the effects of the width of the incident neutral beam removed. Nevertheless, the energy bin shape of the IBEX-Lo sensor prototype remains well defined down to 10 eV and the deviation from the shape calculated using a mono-energetic neutral beam is entirely due to the predicted width of 15% of the primary energy in the energy range used.

Conclusion

We built a portable device to neutralize an ion beam. The device may easily be mounted into the existing calibration facilities and requires no additional resources for operation, except high voltages. A neutral hydrogen beam over a wide energy range of 10–1000 eV was produced. The ion-beam neutralizer was successfully used for the characterization of the neutral interstellar composition experiment (NICE) [24] and the prototype of the IBEX-Lo sensor [16] of the Interstellar Boundary Explorer (IBEX) [8].

Acknowledgment

This work was supported by the Swiss National Science Foundation.

References

[1] Fahr H-J 2004 Global structure of the heliosphere and interaction with the local interstellar medium: three decades of growing knowledge *Adv. Space Res.* **34** 3–13
[2] Thomas G E 1978 The insterstellar wind and its influence on the interplanetary environment *Ann. Rev. Earth Planet* **6** 173–204
[3] Zank G P and Pauls H L 1996 Modelling the heliosphere *Space Sci. Rev.* **78** 95–106
[4] Gruntman M, Roelof E C, Mitchell D G, Fahr H J, Funsten H O and McComas D J 2001 Energetic neutral atom imaging of the heliospheric boundary region *J. Geophys. Res.* **106** 15767–81
[5] Wurz P 2000 Detection of energetic neutral particles *The Outer Heliosphere: Beyond the Planets* (Katlenburg-Lindau: Copernicus Gesellschaft eV) pp 251–88
[6] Witte M, Rosenbauer H, Keppler E, Fahr H, Hemmerich P, Lauche H, Loidl A and Zwick R 1992 The interstellar neutral-gas experiment on ULYSSES *Astron. Astrophys.* **92** 333–48
[7] Moore T E *et al* 2000 The low-energy neutral atom imager for IMAGE *Space Sci. Rev.* **91** 155–95
[8] McComas D J *et al* 2004 The interstellar boundary explorer (IBEX) *Physics of the Outer Heliosphere: 3rd Int. IGPP Conf.* ed V Florinski, N V Pogorelov and G P Zank (*AIP Conf. Proc.* vol 719) (New York: AIP) pp 162–81
[9] Ghielmetti A G, Balsiger H, Bänninger R, Eberhardt P, Geiss J and Young D T 1983 Calibration system for satellite and rocket-borne ion mass spectrometers in the energy range from 5 eV/q to 100 keV/q *Rev. Sci. Instrum.* **54** 425–36
[10] Marti A, Schletti R, Wurz P and Bochsler P 2001 New calibration facility for solar wind plasma instrumentation *Rev. Sci. Instrum.* **72** 1354–60
[11] Utterback N G and Miller G H 1961 Fast molecular nitrogen beam *Rev. Sci. Instrum.* **32** 1101–6
[12] Stephen T M, van Zyl B and Amme R C 1996 Generation of a fast atomic-oxygen beam from O^- ions by resonant cavity radiation *Rev. Sci. Instrum.* **67** 1478–82
[13] Eckstein W 1981 Charge fractions of reflected particles *Inelastic Particle–Surface Collisions (Chemical Physics* vol 17*)* (Berlin: Springer) pp 157–83
[14] Losch A and Niehus H 1999 Structure analysis of the KBr(100) surface—an investigation with a new method for surface analysis on insulators *Surf. Sci.* **420** 148–56
[15] Losch A and Niehus H 1999 NICASS—a new method for surface structure analysis *Phys. Stat. Sol.* **173** 117–21
[16] Wieser M 2005 Detection of energetic neutral atoms and its application to heliospheric science *PhD Thesis* University of Bern
[17] Stephen T M and Pecko B L 1998 Absolute calibration of a multichannel plate detector for low energy O, O^-, and O^+ *Rev. Sci. Instrum.* **71** 1355–9
[18] Peko B L and Stephen T M 2000 Absolute detection efficiencies of low energy H, H^-, H^+, H_2^+, and H_3^+ incident on an multichannel plate detector *Nucl. Instrum. Methods* B **171** 597–604
[19] Oberheide J, Wilhelms P and Zimmer M 1987 New results on the absolute ion detection efficiencies of a microchannel plate *Meas. Sci. Technol.* **8** 351–4
[20] Gao R S, Gibner P S, Newman J H, Smith K A and Stebbings R F 1984 Absolute and angular efficiencies of a microchannel-plate position-sensitive detector *Rev. Sci. Instrum.* **55** 1756–9
[21] Wieser M, Wurz P, Brüning K and Heiland W 2002 Scattering of atoms and molecules off a magnesium oxide surface *Nucl. Instrum. Methods* B **192** 370–80
[22] Taglauer E 1990 Surface cleaning using sputtering *Appl. Phys.* A **51** 238–51
[23] Jans S, Wurz P, Schletti R, Brüning K, Sekar K, Heiland W, Quinn J and Leuchter R E 2001 Negative ion production by surface ionization at barium zirconate surface *Nucl. Instrum. Methods* B **173** 503–15
[24] Wieser M, Wurz P, Bochsler P, Moebius E, Quinn J, Fuselier S A, Ghielmetti A, DeFazio J N, Stephen T M and Nemanich R J 2005 NICE: an instrument for direct mass spectrometric measurement of interstellar neutral gas *Meas. Sci. Technol.* **16** 1667–76